

Viscoelasticity of 2D liquids quantified in a dusty plasma experiment

Yan Feng,* J. Goree, and Bin Liu

Department of Physics and Astronomy, The University of Iowa, Iowa City, Iowa 52242

(Dated: November 12, 2018)

The viscoelasticity of two-dimensional liquids is quantified in an experiment using a dusty plasma. An experimental method is demonstrated for measuring the wavenumber-dependent viscosity, $\eta(k)$, which is a quantitative indicator of viscoelasticity. Using an expression generalized here to include friction, $\eta(k)$ is computed from the transverse current autocorrelation function (TCAF), which is found by tracking random particle motion. The TCAF exhibits an oscillation that is a signature of elastic contributions to viscoelasticity. Simulations of a Yukawa liquid are consistent with the experiment.

PACS numbers: 52.27.Lw, 52.27.Gr, 66.20.-d, 83.60.Bc

Two-dimensional (2D) physical systems include electrons on a liquid helium surface [1], colloids [2], granular fluids [3], and dusty plasmas [4]. In experiments and simulations, elastic properties, such as transverse waves [5, 6], and transport properties, such as viscosity η [7–9], have been studied.

Viscoelasticity is a property of materials that exhibit both viscous and elastic characteristics [10]. One usually thinks of viscous properties for liquids and elastic properties for solids, but most materials are viscoelastic and exhibit both. These include, for example polymers, human tissue, and hot metal [10]. In general, liquids exhibit elastic effects especially at short length or time scales [11], but viscous effects at long length or time scales.

To quantify viscoelasticity, one often uses the frequency-dependent viscosity $\eta(\omega)$ [12], which tends toward the static viscosity, η , as $\omega \rightarrow 0$. The $\eta(\omega)$ is easily measured in three-dimensional (3D) liquids using rheometers and viscometers [12], but not in most 2D liquids.

Besides $\eta(\omega)$, the wavenumber-dependent viscosity, $\eta(k)$, has been used by theorists to quantify the viscoelastic character [13–17]. They have recently developed ways of computing $\eta(k)$ from the trajectories of random motion of molecules [16, 17]. However, until now, there have been no experimental measurements in any physical systems known to us of $\eta(k)$ that exploit this new analysis method. One difficulty in using this method in an experiment is that it requires, as its inputs, the positions x_i and velocities v_i of N individual molecules or particles as they move about randomly. In this Letter, we will use an experimental system, dusty plasma, that allows observing these inputs directly.

Here we further develop a method for computing $\eta(k)$, generalizing it for multiphase systems like dusty plasma. As was originally developed for 3D molecular dynamics (MD) simulations, the method begins with computing the normalized transverse current autocorrelation function [16, 17] (TCAF), which is defined as

$$C_T(k, t) = \langle j_y^*(k, 0) j_y(k, t) \rangle / \langle j_y^*(k, 0) j_y(k, 0) \rangle, \quad (1)$$

where $j_y(k, t) = \sum_{i=1}^N v_i^y(t) \exp[ikx_i(t)]$ is the transverse current, with the vector k parallel to the x axis. Then, $\eta(k)$ can be calculated [16, 17] through $\eta(k)/\rho = 1/(k^2 \Phi)$, where Φ is the area under the normalized TCAF. This equation can be derived, assuming that the viscosity is a valid transport coefficient, either from the hydrodynamic Navier-Stokes equation or from linear response theory [17]. Here, we generalize this equation using $\partial \mathbf{j}(\mathbf{r}, t) / \partial t - (\eta/\rho) \nabla^2 \mathbf{j}(\mathbf{r}, t) + \nu_f \mathbf{j}(\mathbf{r}, t) = 0$, a Navier-Stokes equation that includes an additional frictional drag force $\nu_f \mathbf{j}(\mathbf{r}, t)$ due to a second phase [7]. This equation is valid in both 2D and 3D systems. Following the method of [17], we find [18]

$$\eta(k)/\rho = ((1/\Phi) - \nu_f)/k^2. \quad (2)$$

Here we will characterize viscoelasticity in an experiment two ways. First, as a signature of elastic effects, we will detect oscillations in the TCAF [14, 16] for large k . Second, we will measure the diminishment of $\eta(k)$ as k increases. This diminishment occurs along with a relative increase of elastic contributions to viscoelasticity, for large k .

Dusty (complex) plasma, is partially ionized gas containing micron-size particles of solid matter [4, 19, 20]. Particles have a charge Q and can be electrically confined in a single horizontal layer where they self-organize with a structure like a crystalline solid [20]. Coulomb repulsion is shielded with a screening length λ_D [21, 22]. The elastic properties of the crystalline solid arise from interparticle repulsion and can be characterized by the phonon spectrum for longitudinal and transverse waves [23], which have a frequency close to the nominal 2D dust plasma frequency ω_{pd} [24]. The solid can be melted, to form a liquid, by laser manipulation [25, 26].

Dusty plasmas are attractive for experimental quantification of viscoelastic effects at a microscopic scale. As in colloids [2] and granular fluids [3], they allow video microscopy to track the x_i and v_i of individual particles. They also provide both elastic and viscous effects. The particles are immersed in a medium that is a rarefied gas that does not overdamp particle motion, unlike

colloids [2] with their solvents.

Dusty plasma experiments, until now, have yielded descriptive presentations of viscoelasticity [27] and demonstrations of the microscopic motion of particles associated with viscoelastic response [28]. In experiments, the static viscosity has been measured [7] and estimated from diffusion observations [29]. However, a quantitative characterization of viscoelasticity, using $\eta(\omega)$ or $\eta(k)$, is lacking from the literature.

A challenge in dusty plasma experiments is that they do not allow direct contact of the suspension with a container. Thus, the viscoelastic response cannot be measured with a rheometer. We overcome this challenge by observing the random particle motion and using Eq. (2) to compute $\eta(k)$. We will do this with experimental data, and confirm our interpretation using a simulation.

Using the apparatus of [30], a plasma was powered by 13.56 MHz, 170 V peak to peak voltages. After the 8.1 μm diameter microspheres were introduced into the plasma (which had an Argon pressure of 14 mTorr), they experienced a damping rate of $\nu_f = 2.4 \text{ s}^{-1}$ [31].

The particles were suspended in a single layer. They self-organized in a triangular lattice [20]. Particle motion was essentially 2D, with negligible out-of-plane displacements. The suspension had a diameter $\approx 52 \text{ mm}$ and contained > 5400 particles. The lattice constant $b = 0.67 \text{ mm}$ corresponds to a Wigner-Seitz radius [24] $a = 0.35 \text{ mm}$.

Particle tracking was done by imaging from the top. For each of four runs, 20 s videos were recorded at 250 frames/s, providing adequate time resolution for the TCAF. The $(36.2 \times 22.6) \text{ mm}^2$ field of view (FOV) included ≈ 2100 particles. We recorded the maximum 5061 frames per run allowed by the 12-bit Phantom v5.2 camera, with a lens that provided a resolution of 0.03 mm/pixel. For each video frame j , we computed [32] the position of the i th particle, $\tilde{x}_{i,j}$. To compute $j_y(k, t)$, we used $x_{i,j} = (\tilde{x}_{i,j-1} + \tilde{x}_{i,j} + \tilde{x}_{i,j+1})/3$ and $v_{i,j}^y = (\tilde{y}_{i,j+1} - \tilde{y}_{i,j-1})/2\delta t$. This finite-difference method reduced errors arising from the high frame rate. Examples of particle trajectories from the experiment are shown in Fig. 1(a). Next, we computed $j_y(k, t)$ and smoothed its time series over five frames before calculating the TCAF, Eq. (1), and finally $\eta(k)$, Eq. (2).

Before melting the suspension, we used the phonon-spectrum method for a lattice [23] to measure $Q/e = -6000$, $\kappa_0 = a/\lambda_D = 0.5$, and $\omega_{pd} = 30 \text{ s}^{-1}$. After melting, we determined T from the mean-square velocity fluctuation [20] yielding $\Gamma = (Q^2/4\pi\epsilon_0 a)/(k_B T) = 68$.

We melted the lattice and maintained a steady kinetic temperature T using laser manipulation [25, 30]. Random kicks were applied by radiation pressure from a pair of 532-nm laser beams that were rastered across the suspension in a Lissajous pattern with frequencies $f_x = 48.541 \text{ Hz}$ and $f_y = 30 \text{ Hz}$. This pattern filled a rectangle larger than the camera's FOV. Along with the

desired random motion, the Lissajous heating method also produces coherent modes [25], which had about 8% of our total kinetic energy for motion in the y direction, similar to [30]. We analyzed half of the FOV, where the temperature was uniform within extremes of $\pm 20\%$.

For comparison to the experiment, we also performed a Langevin MD simulation [33–36] of a 2D Yukawa liquid to mimic our experiment. Using periodic boundary conditions and 4096 particles, the equation of motion Eq. (3) of [33] was integrated, yielding particle trajectories, Fig. 1(b). The simulation parameters $\Gamma = 68$, $\kappa_0 = 0.5$, and $\nu_f/\omega_{pd} = 0.08$ match the experimental values. To improve statistics, the simulation was run much longer, $\omega_{pd}t = 22\,300$, than the experiment $\omega_{pd}t = 607$. To validate our Langevin MD simulation, we also performed a frictionless MD simulation [8] and calculated $\eta(k)$ as in Eq.(2) but with $\nu_f = 0$; we found that the results for $\eta(k)$ for the two types of simulations agree. In addition to computing $\eta(k)$, we also computed the static viscosity η using the Green-Kubo relation, Eq. (3) of [8]. The latter assumes that the shear-stress autocorrelation function decays significantly faster than $1/t$, which we verified.

Experimental results for the TCAF, Fig. 2(a), reveal elastic properties in the viscoelastic regime for this liquid. The TCAF computed from Eq. (1) exhibits an initial decay followed by oscillations around zero [14, 16], for $kb = 3.26$ in Fig. 2(a). Such oscillations typically indicate that the selected wavenumber corresponds to the viscoelastic regime. The TCAF is a time series; we also calculate its frequency spectrum, shown in the inset of Fig. 2(a). (This frequency spectrum can also be used in generating a phonon spectrum [11]). The spectrum features a prominent peak at non-zero frequency. This peak is a signature of shear elasticity; it would be absent in a viscous regime. To our knowledge, the TCAF time series has not previously been reported for dusty plasma experiments as an indicator of viscoelasticity.

Simulation results, Fig. 2(b), exhibit features in the TCAF and its spectrum [14] similar to those in the experiment. This agreement between experiment and simulation lends confidence to our use of the TCAF as a quantitative indicator of viscoelasticity in an experimental system.

For wavenumbers much smaller than those shown in Fig. 2, i.e., for very long wavelengths, we would expect viscous behavior characterized by a simple decay of the TCAF with no oscillations. This hydrodynamic regime has been well studied in simulations and theory [37]. Observing it requires a sufficiently large system. One of the attractions of our physical system is that it allows direct observation of motion at an atomistic scale. Thus, we use it here to observe the viscoelastic regime (at small wavelengths), not the purely viscous hydrodynamic regime.

As our chief result, our experimentally measured wavenumber-dependent viscosity, $\eta(k)$, is presented

quantitatively in Fig. 3(a). We observe that $\eta(k)$ diminishes as k increases. Physically, this trend indicates that dissipative or viscous effects diminish at shorter length scales. At these shorter length scales, elasticity has a greater effect.

Since previous experiments are not available for quantitative comparison, we compare our experimental results to the Langevin simulation, Fig. 3(b). We note that $\eta(k)$ exhibits the same downward trend and similar quantitative values in the experiment and the simulations. For both the experiment and simulation, we present results for $\eta(k)$, computed using Eq. (2), for the viscoelastic regime, i.e., $k > 1/b$. For each k , the infinite time limit for the integration of Φ was replaced with t_I , the time of the first upward zero-crossing of TCAF time series (Fig. 2). This integration limit retains both the viscous effects at short time and the elastic effects within the first negative peak.

Noise in the experimental results arose from the finite amount of current data used to compute the TCAF. To verify that this accounts for the scatter in the experimental $\eta(k)$ in Fig. 3(a), we repeated the simulation with a shorter time, matching the experiment not only in duration but also in particle number. This test shows, in Fig. 3(b), that scatter arises from the finiteness of the $j_y(k, t)$ data to the same extent as in the experiment. In both the experiment and in the shorter simulation, a few TCAF curves were too noisy to analyze, with a lack of a well-defined upward zero-crossing; the corresponding few data points are omitted from Fig. 3.

We fit $\eta(k)$ in Fig. 3 to the same empirical Padé approximant used originally for MD simulations of 3D liquids of hard spheres [13] and water [16]. This approximant, $\eta(k) \propto (1 + \alpha k^2)^{-1}$, apparently has never been applied for 2D liquids. We found that this form fits both our experimental and simulation data in Fig. 3 as well as the scatter allows. However, a simple power law does not fit the $\eta(k)$ data as well.

In addition to finding that our $\eta(k)$ fits the Padé approximant, we also find in Fig. 3(b), that it extrapolates as $k \rightarrow 0$ to the static viscosity η [16]. In this test, we found η using the Green-Kubo relation [8] with our Langevin simulation; and this result, shown as a star in Fig. 3(b), agrees with previous simulations that used different methods [8, 9].

In conclusion, we performed an experiment to quantify viscoelasticity of 2D liquids using the TCAF and $\eta(k)$. We did this using measurements of random particle motion in a dusty plasma, which is a frictional system. We generalized a method of calculating $\eta(k)$ by including the friction in the Navier-Stokes equation; and we presented an experimental demonstration of this method. Our experimental results for $\eta(k)$ show that it diminishes with increasing k that can be modeled as $\propto (1 + \alpha k^2)^{-1}$, which compares well with simulation results.

This work was supported by NSF and NASA. We

thank Zhonghan Hu for helpful discussions.

* Electronic address: yan-feng@uiowa.edu

- [1] C. C. Grimes and G. E. Adams, Phys. Rev. Lett. **42**, 795 (1979).
- [2] C. A. Murray, W. O. Sprenger, and R. A. Wenk, Phys. Rev. B **42**, 688 (1990).
- [3] P. M. Reis, R. A. Ingale, and M. D. Shattuck, Phys. Rev. Lett. **96**, 258001 (2006).
- [4] G. E. Morfill and A. V. Ivlev, Rev. Mod. Phys. **81**, 1353 (2009).
- [5] S. Nunomura, D. Samsonov, and J. Goree, Phys. Rev. Lett. **84**, 5141 (2000).
- [6] Z. Donkó, P. Hartmann, G. J. Kalman, Phys. Rev. E **69**, 065401(R) (2004).
- [7] V. Nosenko and J. Goree, Phys. Rev. Lett. **93**, 155004 (2004).
- [8] B. Liu and J. Goree, Phys. Rev. Lett. **94**, 185002 (2005).
- [9] Z. Donkó, J. Goree, P. Hartmann, and K. Kutasi, Phys. Rev. Lett. **96**, 145003 (2006).
- [10] R. Lakes, *Viscoelastic Materials*, 1st ed. (Cambridge University Press, Cambridge, 2009).
- [11] V. Nosenko, J. Goree, and A. Piel, Phys. Rev. Lett. **97**, 115001 (2006).
- [12] T. G. Mason and D. A. Weitz, Phys. Rev. Lett. **75**, 2770 (1995); R. F. Berg, M. R. Moldover, and G. A. Zimmerman, Phys. Rev. E **60**, 4079 (1999).
- [13] W. E. Alley and B. Alder, Phys. Rev. A **27**, 3158 (1983).
- [14] U. Balucani, R. Vallauri, and T. Gaskell, Phys. Rev. A **35**, 4263 (1987).
- [15] B. J. Palmer, Phys. Rev. E **49**, 359 (1994).
- [16] U. Balucani, J. P. Brodholt, P. Jedlovsky, and R. Vallauri, Phys. Rev. E **62**, 2971 (2000).
- [17] Z. Hu and C. J. Margulis, J. Phys. Chem. B **111**, 4705 (2007).
- [18] See EPAPS Document No. XXXXXX for the derivation of Eq. (2). For more information on EPAPS, see <http://www.aip.org/pubservs/epaps.html>.
- [19] A. Melzer, A. Homann, and A. Piel, Phys. Rev. E **53**, 2757 (1996).
- [20] Y. Feng, J. Goree, and B. Liu, Phys. Rev. Lett. **100**, 205007 (2008).
- [21] U. Konopka, G. E. Morfill, and L. Ratke, Phys. Rev. Lett. **84**, 891 (2000).
- [22] O. S. Vaulina *et al.*, Phys. Lett. A **372**, 1096 (2008).
- [23] S. Nunomura, S. Zhdanov, D. Samsonov, and G. Morfill, Phys. Rev. Lett. **94**, 045001 (2005).
- [24] G. J. Kalman, P. Hartmann, Z. Donkó, and M. Rosenberg, Phys. Rev. Lett. **92**, 065001 (2004).
- [25] V. Nosenko, J. Goree, and A. Piel, Phys. Plasmas **13**, 032106 (2006).
- [26] M. Wolter and A. Melzer, Phys. Rev. E **71**, 036414 (2005).
- [27] S. Ratynskaia *et al.*, Phys. Rev. Lett. **96**, 105010 (2006).
- [28] C. L. Chan and L. I, Phys. Rev. Lett. **98**, 105002 (2007).
- [29] U. Konopka *et al.*, Phys. Rev. E **61**, 1890 (2000).
- [30] B. Liu and J. Goree, Phys. Rev. Lett. **100**, 055003 (2008).
- [31] B. Liu, J. Goree, V. Nosenko, and L. Boufendi, Phys. Plasmas **10**, 9 (2003).
- [32] Y. Feng, J. Goree, and B. Liu, Rev. Sci. Instrum. **78**,

- 053704 (2007).
- [33] Y. Feng, B. Liu, and J. Goree, Phys. Rev. E **78**, 026415 (2008).
- [34] L. J. Hou, A. Piel, and P. K. Shukla, Phys. Rev. Lett. **102**, 085002 (2009).
- [35] O. S. Vaulina *et al.*, Phys. Rev. Lett. **103**, 035003 (2009).
- [36] T. Ott and M. Bonitz, Phys. Rev. Lett. **103**, 195001 (2009).
- [37] J. P. Hansen and I. R. McDonald, *The Theory of Simple Liquids*, 2nd ed. (Elsevier Academic Press, Amsterdam, 1986).

FIG. 1: (Color online) Particle trajectories in a 2D liquid, with color representing time. To illustrate the random particle motion, (a) shows $\approx 10\%$ of the spatial region we analyzed, for a duration $60 \omega_{pd}^{-1}$ which is about $\approx 10\%$ of one movie, i.e., one run in the experiment, while (b) is a part of a Langevin MD simulation, shown over the same time interval.

FIG. 2: Transverse current autocorrelation function (TCAF) in the 2D liquid computed using Eq. (1) for (a) the experiment at $kb = 3.26$, and (b) the Langevin MD simulation at $kb = 3.28$. At short times, the TCAF decays due to viscous effects, while at longer times (after its first positive zero crossing, t_I) it oscillates due to elastic effects. The frequency spectrum for each TCAF, shown in the insets, reveals a peak that is a signature of the elastic contribution to viscoelasticity. These results are different from the pure monotonic decay of TCAF and its spectrum that would be observed in a purely viscous regime. (Here, b is the lattice constant measured before melting.)

FIG. 3: (Color online) The wavenumber-dependent viscosity $\eta(k)$ of the 2D liquid, computed using Eq. (2) for (a) the experiment and (b) simulations of two sizes. We find that $\eta(k)$ diminishes with k , which is a signature of viscoelastic effects. The size of the smaller simulation mimics the size of the experiment; comparing them reveals that the scatter of the experimental data (a) arises from the data size. In (b), the Green-Kubo (static) viscosity η is indicated by a star symbol. Here, the kinematic viscosity $\eta(k)/\rho$ and wavenumber k are normalized to be dimensionless.

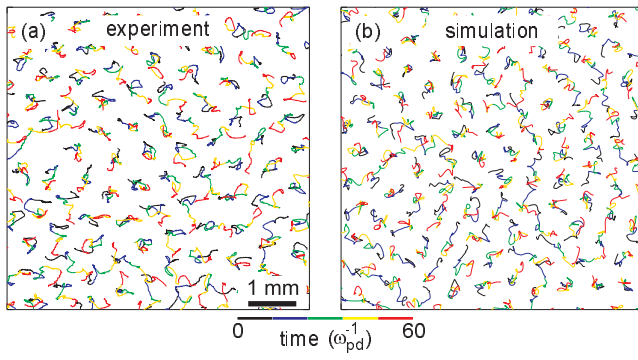


Fig. 1

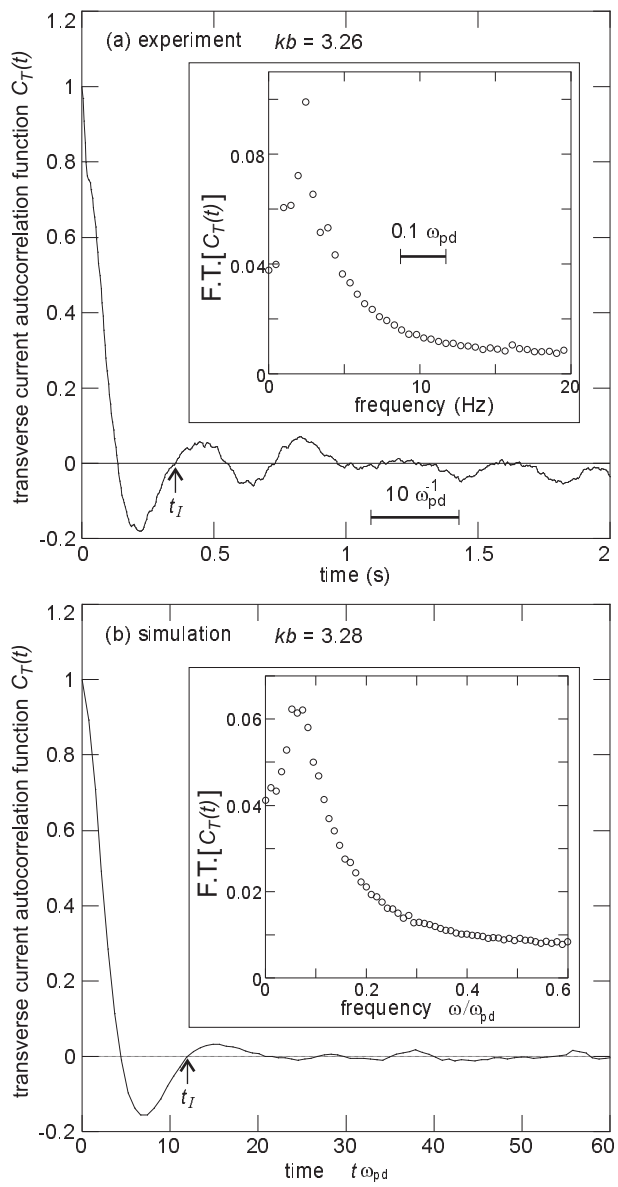


Fig. 2

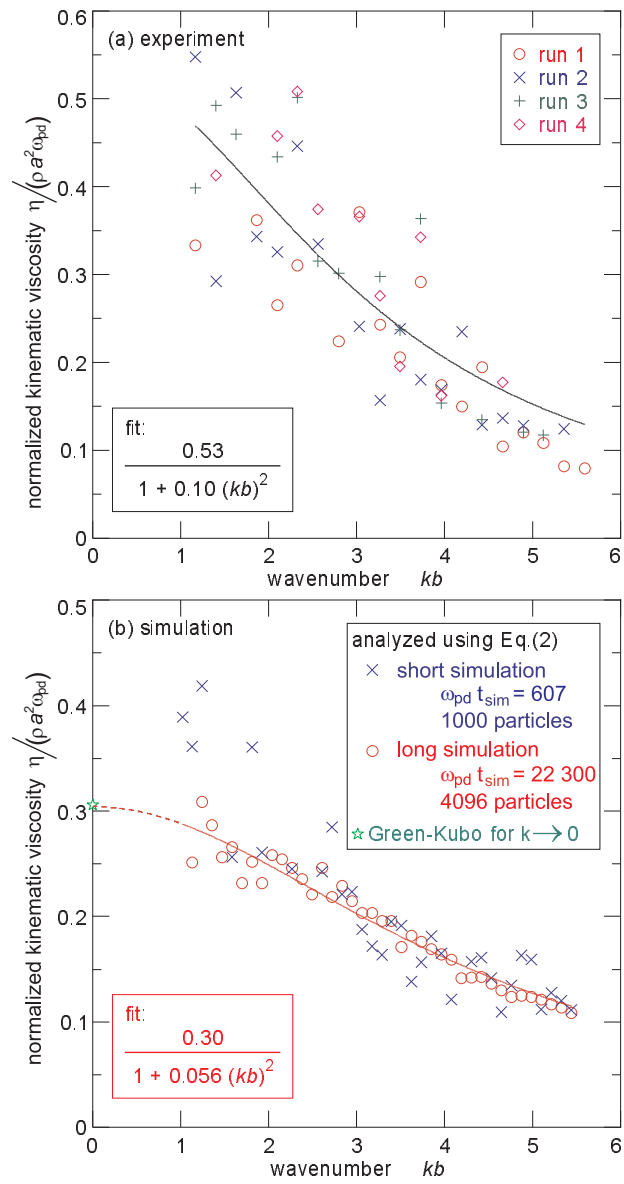


Fig. 3